

Sonic Boom Analysis of Meteorite at Hypersonic Speeds in Earth Atmosphere

YAMASHITA, Rei^{1*} ; SUZUKI, Kojiro¹

¹Graduate School of Frontier Sciences, The University of Tokyo

The sonic boom followed by the passage of shock waves may cause serious damage on the ground, when a meteorite falls at hypersonic speeds as experienced at the Chelyabinsk meteorite event in February 2013. Therefore, it is important to evaluate the sonic boom generated by the meteorite. In this study, the prediction method of the sonic boom developed in the aeronautical engineering is applied to the case of the meteorite. The nature of the sonic boom propagation in the earth atmosphere is evaluated by the whole-domain simulation technique, which is based on the computational fluid dynamics in the domain bounded by the flying object and the ground (R. Yamashita and K. Suzuki, APISAT2013, No. 02-05-3). The flowfield around the sphere with 20 m diameter is numerically obtained by solving the three dimensional Navier-Stokes equations with the gravity term. The earth's atmospheric model is based on the international standard atmosphere (ISO 2533:1975). The flight Mach number is 10 (about 3 km/s), the flight altitude is 10 km and the flight condition is the steady level flight. The computational grid is constructed by rotating the two dimensional grid about the body axis and the number of the grid points is about 5.5 million. After the numerical calculation is conducted by using the initial grid, the calculation is performed again with the adaptive grid reconstructed to align the bow shock wave to avoid the artificial smearing of the shock wave. For computational efficiency, the domain is divided into several sectors from the body to the ground. The shape of the meteorite is approximated as a sphere and the axi-symmetric flowfield is assumed in the sector near the body. The numerical fluxes are evaluated by SHUS scheme (E. Shima and T. Jounouchi, NAL SP, pp.7-12, 1997) with the third order accuracy by MUSCL interpolation technique. The time integration is conducted by MFGS (E. Shima, proceedings of 29th Fluid Dynamic Conference, pp.325-328, 1997) method. The gravity term is added to the governing equations as a source term.

The flowfield around the sphere is composed of the bow shock wave in front of the body and the trailing shock wave in the wake. Both the waves propagating downward are merged into a single wave at 8 km altitude. In such case, the sonic boom sounds only once, while the sonic boom generated by a supersonic airplane creates explosive sounds twice without merging of the shock waves. It is reported that Chelyabinsk meteorite has been broken into three big pieces and the sonic boom sounds three times at the ground (NHK COSMIC FRONT, June 2013). Hence, the number of the pieces is equal to that of the sound of explosion. This fact seems consistent with the present simulation result. The pressure rise across the shock wave decreases with the distance from the body because of the geometric spreading. In the actual earth's atmosphere, however, the rate of decrease becomes smaller near the ground, because the atmospheric pressure and temperature increase toward the ground. Assuming the pressure augmentation factor of 1.9 at the reflection of the shock wave at the ground, the peak pressure rise is estimated at about 1.5 kPa, which is 63 times as large as the maximum allowable pressure rise (24 Pa) determined in the environmental regulation for the supersonic airplane. In the case of the Chelyabinsk meteorite, the pressure rise is estimated at 3.2 ± 0.6 kPa (Nature 12741) from the observation of the damage of the glass windows there. Although the numerical condition is not the same as the actual flight condition of the meteorite, the pressure rise due to the passage of a meteorite at hypersonic speeds is expected to be in the order of 1 kPa or higher.

As mentioned above, the prediction method developed in the aeronautical engineering has a great potential to predict the flight condition, say, the size, altitude and Mach number, from the magnitude of the sonic boom measured on the ground by conducting the parametrical study.

Keywords: Sonic Boom, Meteorite, Hypersonic Flow, CFD, Shock Wave

The brightness and the color temperature of the Chelyabinsk bolide

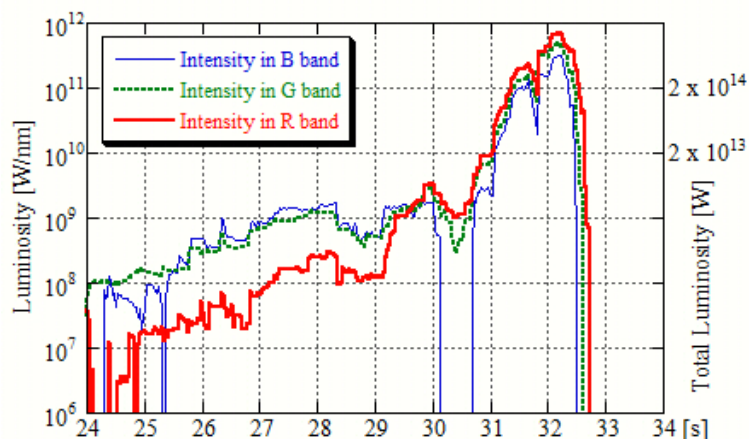
YANAGISAWA, Masahisa^{1*}

¹Univ. Electro-Communications

The bolide explosion on Feb. 15, 2013 over Chelyabinsk, Russia was the next most violent to the probable bolide explosion in Tunguska, Siberia in 1908. It was recorded by many dashboard movie cameras in a wide area around the city, and the movies are released on the Internet. We analyzed one of them and obtained the lightcurves of the bolide for three colors (see the figure for the temporal variations of the brightness). More than 95% of the radiant energy in the visible wavelengths was released in its flare-up for about 2 seconds. The luminosity ratios among the R (red), G (green), and B (blue) color bands are consistent with the 3500 K black-body radiation during the flare, while the pre-flare bolide was greenish-blue in color and the ratios do not agree to the black-body spectra. The maximum luminosity was 1.0×10^{15} W. The impact energy is estimated to be 1.9×10^{15} J or 450 kton in TNT equivalent ($1 \text{ kton} = 4.185 \times 10^{12}$ J), based on an empirical formula for the radiant efficiency of bolides. The lightcurves and the impact energy almost agree to the results reported thus far.

Figure caption: Temporal variations of the source luminosities of the bolide in logarithmic scales. The thick (red), dotted (green), and thin (blue) lines correspond to the RGB color bands. The calculated intensities are negative in the periods without plot. The vertical scale on the right side shows the luminosity integrated over the wavelengths assuming 3500 K black body radiation. Seconds of 3:20 on Feb. 15, 2013 (UT) are shown in abscissa.

Keywords: bolide, meteoroid impact, small solar system objects, Chelyabinsk, Space guard, meteorites



Statistical distribution of the solar system dusts by meteor head echo observations with the large-aperture radar

ABE, Shinsuke^{1*} ; KERO, Johan² ; NAKAMURA, Takuji³ ; FUJIWARA, Yasunori⁴ ; WATANABE, Jun-ichi⁵

¹Department of Aerospace Engineering, College of Science and Technology, Nihon University, ²Swedish Institute of Space Physics (IRF), ³National Institute of Polar Research (NIPR), ⁴Nippon Meteor Society, ⁵National Astronomical Observatory of Japan

A meteor head echoes is caused by radio waves scattered from the intense region of the plasma surrounding and co-moving with a meteoroid during atmospheric entry at about 70-130 km altitude. Meteor head echo observations were carried out using the high-power large-aperture (HPLA) Kyoto university Shigaraki middle and upper atmosphere (MU) radar in Japan (34.85deg N, 136.10deg E). Since 2009 the atmospheric trajectories and interplanetary orbital elements have been derived by the MU radar meteor head echoes (e.g.; Kero et al. (2012); Kero et al. (2011)). Approximately 120,000 orbital elements of meteors with excellent accuracy were obtained until January 2014. Typical error for velocity and semi-major axis are 0.3 km/s and 0.1 AU, respectively. Such a huge number of meteoroid orbits with the precise orbital accuracy has not been observed before. Here we report some results obtained by the statistical analysis of the database, such as orbital distributions and associations of comets and asteroids.

Keywords: meteors, dusts, meteoroids, comets, asteroids, MU radar

Laboratory experiment simulating Martian surface observation with submillimeter-wave polarimetric radiometry

ARIMURA, Taketo^{1*} ; OCHIAI, Satoshi² ; KIKUCHI, Kenichi² ; KITA, Kazuyuki³ ; KASAI, Yasuko²

¹Graduate School of Science and Engineering, Ibaraki University, ²National Institute of Information and Communications Technology, ³Faculty of Science, Ibaraki University

Energies and materials exchange between the ground and atmosphere on Mars play important roles in the Martian general circulation. It is necessary to observe the spatial and temporal variability of the Martian surface from orbiter. However, it has been quite difficult to continually monitor the Mars surface in optical observation due to opaqueness of the Martian dust. Millimeter/submillimeter radiometers enable to observe the Martian surface through dust, though such measurement has never been conducted in planetary exploration. We assess the effectiveness of this observation method by laboratory experiment.

By observing millimeter/submillimeter emission from the Martian surface in several emission angles and two polarizations, we can derive physical temperatures, permittivity and roughness of the surface from brightness temperatures. In order to estimate each property from polarized brightness temperatures, we need to know relationship between emissivity or/and reflectivity in millimeter/submillimeter wave region and the parameters of surface.

We developed an experiment system to examine millimeter/submillimeter scattering and emission characteristics of the simulated Martian surface in a chamber. Measurement samples in the chamber are coolable at Martian surface temperature. The chamber is designed to measure emission of samples using a receiver and reflection of samples using a transmitter and a receiver. We can also obtain arbitrary-polarized emission with arbitrary incident angle by controlling mirrors in our system.

To discuss relationship between emission and surface parameters on the Martian surface, it is necessary to know influences of permittivity and surface roughness on the reflectivity. Therefore, we measured reflectance of Acrylic plate and Alumina grain at millimeter/submillimeter waves region. We discuss effects of permittivity and roughness on measured reflectivity of measurement samples in known polarization and incident angle. Moreover, we retrieve the permittivity and the roughness of sample from measured reflectivity. Using this measurement results, we expect a step closer to explanation of relationship between emission and surface parameters in the Martian surface at millimeter/submillimeter waves region.

Keywords: Mars, surface observation, submillimeter-wave

Scientific importance and possibility of HCN detection in Enceladus plumes by ALMA

KODAMA, Kenya^{1*} ; SEKINE, Yasuhito¹ ; IINO, Takahiro² ; SAIGO, Kazuya⁶ ; KASAI, Yasuko³ ; SAGAWA, Hideo⁴ ; MAEZAWA, Hiroyuki⁵

¹Dept. Complexity Sci. and Engr. Univ. of Tokyo, ²Solar-Terrestrial Environment Laboratory, Graduate school of science, Nagoya University, ³Senior Researcher Global Environment Division National Institute of Information and Communications, ⁴National Institute of Information and Communications Technology, ⁵Department of Physical Science Osaka Prefecture University, ⁶National Astronomical Observatory of Japan

Saturn's icy moon, Enceladus, exhibits ongoing geological activities, including eruption of water-rich plumes from warm fractures near the south-pole region. These geological activities together with the findings of Na-rich salts in the plumes suggest the presence of an interior liquid ocean beneath the icy crust. This demonstrates that Enceladus' plumes provide a unique opportunity to investigate the chemical composition of oceanic water, possible geochemical reactions, and habitability of the icy moon. However, due to limitations of in-situ measurements of the plumes by the Cassini spacecraft, it is not able to identify or quantify some key molecules, which could probe physical and chemical conditions of the ocean.

Here we discuss scientific importance and possibility of detection of HCN in the plumes by large ground-based, sub-millimeter telescope, ALMA. Because HCN is one of the fundamental materials contained in icy planetesimals in the outer solar system, and because it readily hydrolyzes in warm water (>50 °C), a lack of HCN suggests that Enceladus' interior would have experienced relatively high temperatures, i.e., a presence of hydrothermal activity. On the other hand, if HCN were present in the plumes, this in turn means that Enceladus would have been cold throughout its history. Given the results of thermal evolution model, the latter case suggests late formation of the Saturnian system (>5 Myr) after CAI formation, which would result in a depletion of short-lived radiogenic heat source in Enceladus.

To evaluate the possibility to detect HCN in the plumes by ALMA, we first estimate a special distribution of H₂O gas density based on results from Cassini's observations and plume eruption modeling. Then, we calculate radiative temperatures of HCN in the field of view of ALMA as a function of HCN concentration. Finally, the upper limit of HCN as a function of observation time will be obtained. For instance, if HCN were not detected within 4-6 hours of observation time, an upper limit of the HCN concentration in the plumes becomes 0.2% relative to water, which is comparable to a typical concentration of HCN in comets. Thus, the ALMA telescope is capable of detecting HCN in Enceladus' plumes within a reasonable observation time, if it were present in an amount comparable to that of comets. In either case whether HCN were present or not, we would be able to constrain geochemical reactions and thermal history of Enceladus as well as the timing of formation of Saturnian system.

Development of SPH: Toward Understanding of Disk-planet Interaction Near the Disk Inner Edge

FUJII, Yuri^{1*} ; IWASAKI, Kazunari¹ ; TSUKAMOTO, Yusuke¹ ; INUTSUKA, Shu-ichiro¹

¹Nagoya University

Recent observations of exoplanets reveal the existence of close-in planets. These planets are thought to form in outer disks and migrate inward because of the disk-planet interaction. If there are disk inner cavities, planets can stop migrating and stay in close-in orbit. Disk evolution is highly affected by these planets. Thus, the understanding of the interaction between disks and close-in planets is crucial. In this study, we develop a numerical scheme to investigate the interaction between disks and planets. Although the grid-based schemes are widely used in this context, there are difficulties in calculating with a disk inner cavity or eccentric planets. These difficulties can be removed by smoothed particle hydrodynamics (SPH) with high accuracy. In this presentation, we will talk about the development of code and the performance evaluation.

Keywords: exoplanet, protoplanetary disk, smoothed particle hydrodynamics

Evolution of a protoplanetary disk and chemical composition of planetesimals

NAGAHARA, Hiroko^{1*}; OZAWA, Kazuhito¹

¹Dept. Earth Planet. Sci., The Univ. Tokyo

We investigate physico-chemical evolution of the proto-solar disk at the early stage by developing a new model that combines physics and chemistry with special interest to temporal and spatial evolution of the disk. Then, we discuss how the composition of planetesimals varies depending on the time and space for their formation including refractory or volatile rich ones.

The basic of the model is a radial advection-diffusion equation, which includes drift and dispersion by turbulence with stochastic diffusion term calculated by the Monte Carlo method and which shows the diffusivity by the viscosity of the disk. The difference from conventional disk models is that the present method stands on the Lagrangean differentiation, and it is able to trace the movement of individual particles.

A considerable amount of materials in the inner regions are transported outward at the early stage ($t < 10^5$ yrs), which is because the surface density is much larger in the inner region at the early stage of the disk evolution. Although the outward flux is large at the early stage, there comes a larger amount of materials from the outer region even within $\sim 10^5$ yrs. The mixing ratio of materials from the inner regions to outer regions is almost unity within several AU all through the disk evolution, suggesting that thermally processed materials and unprocessed materials were mixed in the inner region of the disk. It is important that the relative abundance of materials from outer regions becomes larger with time, which implies that planetesimals formed within several AU at the early stage of the disk evolution consists partly of materials initially located at the inner regions and partly from outer regions, but those formed at the later stage contain more abundant low materials transported from the outer regions.

The mixing ratio of materials from the inner and outer regions is almost unity at the early stage but the fraction of materials from the outer regions increases with time. Combining the information about the maximum temperature that the particles experienced, we can constrain that early differentiated planetesimals such as the parent body of angrites and planetesimals with refractory-rich compositions such as CV chondrites were formed at the inner region of the disk in $\sim 10^5$ yrs. On the other hand, planetesimals for other carbonaceous chondrites or ordinary chondrites that are depleted in sulfur were formed later, possibly at $\sim 10^6$ yrs.

Keywords: protoplanetary disk, chemical evolution, dust movement

Simulating global dust coagulation with grain charging

OKUZUMI, Satoshi^{1*} ; TANAKA, Hidekazu²

¹Graduate School of Science and Engineering, Tokyo Institute of Technology, ²Institute of Low Temperature Science, Hokkaido University

Growth of dust particles by collisions is the initial step of planet formation. Conventionally, the theory of dust coagulation in protoplanetary disks assumed electrically neutral dust particles, but in reality dust in the disks is likely to be charged given that the disks are ionized by cosmic rays and stellar X-rays. In our previous work (Okuzumi 2009; Okuzumi et al. 2011a,b), we extensively studied the role of grain charging in protoplanetary dust growth, and concluded that dust growth stalls at its early stage because of the excessively large (negative) charges carried by small dust aggregates. We also predicted that this "charge barrier" could be overcome (albeit on a very long timescale) if dust in the disks is globally transported by radial drift and turbulent diffusion.

The purpose of the present work is to demonstrate the breakthrough of the charge barrier in a global setup. In order to do this, we have developed a new simulation code for global dust coagulation including the effect of grain charging. The new code is based on a previous code for planetesimal formation (Brauer et al. 2008; Okuzumi et al. 2012) but now calculates charging and Coulomb repulsion of dust particles at each location in a disk consistently with the particle size distribution at the same location. To verify the code, we perform some test simulations and compare them with the prediction from our previous theory.

Keywords: dust, charging, planet formation, protoplanetary disk

N-body simulations of Rubble pile Collisions in Tidal fields

HYODO, Ryuki^{1*} ; OHTSUKI, Keiji¹

¹Kobe University, Graduate School of Science

We examine collisional disruption of gravitational aggregates in the tidal environment by using local N-body simulations. We find that outcomes of such collision largely depend on impact velocity, direction of impact, and radial distance from the planet. In the case of a strong tidal field corresponding to Saturn's F ring, collisions in the azimuthal direction is much more destructive than those in the radial direction. Numerical results of collisions sensitively depend on impact velocity, and complete disruption of aggregates can occur even in impacts with velocity much lower than their escape velocity. In such low-velocity collisions, deformation of colliding aggregates plays an essential role in determining collision outcomes, because the physical size of the aggregate is comparable to its Hill radius. On the other hand, the dependence of collision outcomes on impact velocity becomes similar to the case in free space when the distance from the planet is sufficiently large. We submitted the results to the *Astrophysical Journal*.

Keywords: rings, satellites, aggregates

An improved fragmentation model on outcome of planetesimal collisions

FUJITA, Tomoaki¹ ; GENDA, Hidenori^{2*} ; KOBAYASHI, Hiroshi³ ; TANAKA, Hidekazu⁴ ; ABE, Yutaka¹

¹Department of Earth and Planetary Science, University of Tokyo, ²Earth-Life Science Institute, Tokyo Institute of Technology, ³Department of Physics, Nagoya University, ⁴Institute of Low Temperature Science, Hokkaido University

Collisions between planetesimals or a planetesimal and a protoplanet are thought to occur frequently in the stage of planet formation, and these planetary bodies grow up through these collisions. However, if destructive collisions between them occur frequently, these bodies break up into fragments rather than promote the growth of them. Therefore, in order to understand the process of the growth for planetesimals and protoplanets, it is important to know the impact conditions under which a collision is destructive. The critical specific impact energy for catastrophic disruption Q_D^* , where the largest remnant has half the target mass, has been well investigated under various conditions so far (Holsapple et al., 2002; Benz & Asphaug, 1999; Leinhardt & Stewart, 2009). Such catastrophic impacts have been regarded as important process for planet formation. The values of Q_D^* which has been referred and used most frequently were calculated by Benz and Asphaug (1999). Although they performed many impact simulations to determine Q_D^* , the resolution of their numerical simulation were quite low and they did not check the resolution convergence of Q_D^* . In addition, recent studies (Kobayashi & Tanaka, 2010; Kobayashi et al., 2010) have suggested that non-disruptive small-scaled impacts were also important to the growth of protoplanets, because these small-scaled impacts are much more frequent than disruptive impacts.

In order to discuss more correctly the growth of planets, a correct value of Q_D^* and the relation between ejecta mass and impact energy for small-scaled impacts should be required. In this thesis, I investigate the resolution dependence of Q_D^* and obtain a correct value of Q_D^* for planetesimal collisions by numerical impact simulations with sufficient resolution. I also investigate small-scaled impacts, and formulate the relation between the ejecta mass and impact energy.

Using the smoothed particle hydrodynamics method (SPH) with self-gravity and without strength, I systematically perform the hydrodynamic simulations of collisions between rocky planetesimals. I consider collisions of 10 km and 100 km rocky targets and various sized impactors under various conditions such as impact velocity, impact angle and resolution.

I found that the value of Q_D^* depended on resolution. This is because distribution ratio of initial impact energy to kinetic and internal energy of a target differs depending on resolution due to shear flows which appears during propagation of shock wave and rarefaction wave and ejection process. This energy distribution ratio, probably also Q_D^* , converges in using 7.5×10^7 particles. The resolution in Benz & Asphaug (1999), where they performed impact simulations with 5×10^4 particles, was insufficient. The Q_D^* obtained by higher-resolution simulations is about a half order of magnitude smaller than that of Benz and Asphaug (1999). This means collisions between planetesimals or a planetesimal and a protoplanet are more destructive than previously thought. I applied improved Q_D^* to the growth of protoplanets using analytical method proposed by Kobayashi et al. (2010). As a result, the mass of the finally formed protoplanet is a half smaller than the case for previous Q_D^* . In addition, I derived the formulation of scaling law representing the relation between ejecta mass and impact energy from small-scaled impacts to destructive impacts. I found that this relation can be scaled by target size, impact energy normalized by Q_D^* , and impact velocity, but it depend on impact angle. With Q_D^* and the scaling law obtained in this study, the final grown mass of a protoplanet is $0.058 M_{earth}$ at 1AU and $0.17 M_{earth}$ at 5 AU, where M_{earth} represents the Earth mass.

Numerical modeling of impact phenomena using iSALE shock physics code

KUROSAWA, Kosuke^{1*}; SENSHU, Hiroki¹; WADA, Koji¹; MIKAMI, Takashi²; HIRATA, Naru³; KAMATA, Shunichi²; ISHIHARA, Yoshiaki⁴; GENDA, Hidenori⁵; NAKAMURA, Akiko⁶; TAKATA, Toshiko⁷

¹PERC, Chitech, ²Dept. of CosmoSciences, Hokkaido Univ., ³Dept. of Computer Sci. & Eng., The University of Aizu, ⁴ISAS, JAXA, ⁵ELSI, Titech, ⁶Dept. of Earth and Planetary Sciences, Kobe University, ⁷Division of Science Education, Miyagi University of Education

iSALE (impact-SALE) is a shock physics code based on the SALE hydrocode (Simplified Arbitrary Lagrangian Eulerian), which is an open code for planetary scientist. iSALE contains a number of option to model impact phenomena of geological materials. The calculation results can be easily visualized and analyzed using included software. A number of ANEOS tables and strength models of geological materials, including water ice, silicate rocks, and iron are also included. We have formed a user community called “ iSALE users group in Japan ” to introduce iSALE to the Japanese society for planetary science and to share information on the usage of iSALE. The URL of our wiki page and the mailing list are as follows.

The URL of the wiki page of iSALE users group in Japan
<https://www.wakusei.jp/~impact/wiki/iSALE/>

Mailing list
isale-users-jp@perc.it-chiba.ac.jp

In the presentation, we show the results of a number of test calculations using iSALE.

We gratefully acknowledge the developers of iSALE, including Gareth Collins, Kai W̄nnemann, Boris Ivanov, Jay Melosh and Dirk Elbeshausen.

Keywords: Hypervelocity impacts, Shock physics code, Hydrocode calculation, Equations of state, strength model, iSALE

Study on fundamental characteristics of penetration dynamics into icy target

NAMBA, Kazuya^{1*} ; SUZUKI, Kojiro²

¹Grad. Sch. Eng., The University of Tokyo, ²GSFS, The University of Tokyo

A penetrator, which penetrates the surface of a planet, a satellite and so on to investigate the interior by high-speed hard landing, is expected to play an important role in the solar system exploration of the future. Comparing to soft lander, penetrator has advantages of consuming less fuels, enabling us to launch multiple probes at a time because of its low mass, and so on. However, probe must survive hard impact in collision, thus no penetrator missions have been successfully achieved so far. The icy object, such as 24 Themis and Europa, is expected to contain organics which serve as the precursor of life in their subsurface. Therefore, the cryo-penetrator, which penetrates the icy object and investigate specimens of subsurface which have not been contaminated by cosmic rays, should have a high importance. For a penetrator into regolith, a fully-developed flyable penetrator has been successfully developed for the Lunar-A mission, though the mission itself has been cancelled. For icy target, however, the number of studies from the engineering viewpoint is quite limited, for example, the conceptual study on CRAF mission to a comet nucleus (Adams et al., NASA CR-177393, 1986). In this study, we investigated the fundamental properties of the penetration dynamics of the cryo-penetrator, by conducting penetration experiments into the target made from H₂O ice.

Penetration experiments were conducted by using a ballistic range in our laboratory. The projectile is accelerated by the compressed air, launched horizontally and crashed into a target body. Impact speed is set from 100 m/s to 300 m/s. Two types of projectile, a needle-like one (iron, size: ϕ 2.45x15mm, mass: 1.71g) and a blunt cone-like one (brass, ϕ 8.4x15mm, 2.33g) are used. Three types of target, pure H₂O ice (size: 270x175x130mm, mass: 5.5kg, density: 0.90g/cm³, porosity: 3%), low purity H₂O ice (150x120x100mm, 1.5kg, 0.75g/cm³, 19%) and an oil clay (155x120x70mm, 2.2kg, 1.7g/cm³) are used. A high-speed camera (frame rate: 2200-8800fps, exposure time: 15 μ s) is used to observe a sequence of events: the free-flight of the projectile, impact, crater formation, penetration, and so on.

We found that the penetration into H₂O ice produces ejecta of icy fragments, which erupt conically immediately after collision, and then produces the jet-like ejecta in the almost perpendicular direction to the surface that continues more than 100 msec. On the other hand, the penetration into clay target produces ejecta outward-conically for duration of a few msec. Moreover, we found that the penetrator tends to be pushed back from the target by the ejecta, since the ice around the projectile has been almost broken into pieces erupting as the ejecta and the penetrator cannot be fixed inside the target without receiving the gripping force from the ice. We also found that eruption was continued even after the projectile has completely bounced from the target. This phenomena is frequently observed when the projectile with a less slender body. In the case of a slender penetrator, however, it is hardly subject to bounce-back. Consequently, a slender shape seems more suitable to the penetrator for icy target. The shape of crater consists of the pit region on the center, the spall region which is a shallow depression on the periphery of the pit, and cracks spread a wide range of target. It is qualitatively consistent with previous researches using bullet shape (e.g. Kato et al., Icarus 113(2) 423-441, 1995., Arakawa, Low Temperature Science 66 113-121, 2008). The pressure at a point of impact is estimated by using the one-dimensional planar impact approximation (Wada, JSIAM 16(4) 19-31, 2006): the result shows that it is beyond the Hugoniot elastic limit (HEL), thus the H₂O ice is expected to behave like fluid in the vicinity of the impact point.

This work is supported by Grant-in-Aid for Scientific Research (B) No. 25289301 of Japan Society for the Promotion of Science.

Keywords: icy object, penetrator, crater, ballistic range

Experimental study of compaction process of powder bed by centrifuge experiment

OMURA, Tomomi^{1*}; KIUCHI, Masato¹; GUETTLER, Carsten²; NAKAMURA, Akiko¹

¹Graduate School of Science, Kobe University, ²Max-Planck-Institute for Solar System Research

Dust aggregates in protoplanetary disk are compacted by dust-dust collisions, ram pressure of the disk gas and self-gravity (Kataoka et al., 2013). At reaccumulation phase of asteroids, porosity of rubble pile and regolith would be determined by collisional pressure and self-gravity.

Relationship of porosity of powder layer and particle's radius is given by (Yu et al., 2003; Kiuchi and Nakamura, 2014)

$$p = p_0 + (1 - p_0) \exp\{-m R_F^{-n}\} \quad (1)$$

where R_F is the ratio between the magnitudes of the van der Waals force between two particles and gravity force on particles, therefore a function of particle radius. p_0 , m , and n are constants. p_0 should be understood as the porosity without any interparticle force.

It is not clear if Eq.1 can be applied for powder layer under different gravity from 1 G. Eq.1 was originally derived for particles at surface, and we don't know to what extent this equation is able to be applied for the interior of planetary bodies, i.e., it has not examined for the porosity evolution of bodies due to the accumulation of new grains and blocks onto the surface. If Eq.1 is applicable to such case, porosity given by Eq.1 should be consistent with the result of the case in which R_F is reduced by increasing the gravity. In this study we perform experiments, under different gravitational accelerations, and we compare the results with Eq.1.

We use silica sand, 60 wt% of grains have sizes ranging from 7.5 μm and 80 μm and fly ash, 60 wt% of grains have sizes ranging from 1 μm and 8 μm . They were sieved into a cylindrical container of diameter 5.8 cm and depth 3 cm. After that, the top part of the bed over the height of the container was leveled off. Porosity of each granular bed is approximately 60 % and 70 %. The experiments were performed at elevated acceleration on a centrifuge to provide 1-18 G and observed with a video camera. In contrast with unidirectional compressive compaction using a piston, centrifugal compaction is capable of applying uniform compressive force at any place of the container without causing any local disturbance (Mizuno et al., 1991). After the materials were compressed, bed height was measured with a laser displacement meter and the difference between the initial bed height and the average bed height after acceleration was calculated.

As a result, it is shown that Eq.1 is consistent with experimental result within 6 % (silica sand) and 5% (fly ash) in porosity when assuming the grain diameter=24 μm and 4.5 μm , respectively. This diameter corresponds to the median of cumulative weight distribution of the grains. Also, the diameter of the small silica sand grains stucked with large grains is close to 24 μm .

Keywords: planetesimal, asteroid, porosity, high gravity, powder and granular material

High velocity impact cratering experiments on ice-sand mixture simulating the surface of icy satellites

TAKANO, Shota^{1*} ; ARAKAWA, Masahiko¹ ; YASUI, Minami²

¹Graduate School of Science, Kobe University, ²Organization of Advanced Science and Technology, Kobe University

It is well known that ice-rock mixtures could be a main component of icy satellites, the surface crust of asteroid Ceres. Ceres' icy crust could be impacted by various asteroids with different components and physical properties will affect the crater morphology. Therefore, we would obtain various information from the investigation of the observed craters such as material properties of impacted asteroids and the internal structures of the icy crust and so on. To conduct these investigation, the laboratory experiments would be necessary to derive such information from the observed crater. Then, we should carry out the cratering experiments on ice, ice-rock mixtures and the layered target.

Impact experiments on ice has been conducted systematically under various conditions. However, the cratering experiments on ice-rock mixture were limited in the impact velocity range and the rock contents. It is necessary to experiment at the velocity higher than 4km/s to apply to craters on Ceres, but it is not done now. Therefore, we made cratering experiments on ice-rock mixtures at the impact velocity higher than 1km/s using the several types of the projectile, and compared them with the pure ice to clarify the effects of rock inclusion on the crater morphology and crater scaling law.

We installed and used a new two-stage light gas gun at Kobe University in 2013. We prepared ice-rock mixture targets simulating Ceres crust which consisted of water ice and quartz sand having a particle size of about 500 μ m, and the quartz content was regulated to be 81 \pm 2wt%. The ice-sand mixture was made in a cylindrical metal container with the height of 5~10cm and the diameter of 15cm. The water-sand mixture was frozen in a freezer with the temperature from -23 $^{\circ}$ C to -15 $^{\circ}$ C. Used spherical projectiles were made of aluminum (2.7g/cm³), titanium (5g/cm³), and zirconium (5.7g/cm³), respectively. We launched projectiles at 1.6~5.1km/s with nylon sabots to use various types of projectiles. To prevent targets from melting, the vacuum chamber was evacuated for insulation. The chamber pressure during the experiments was from 200 to 230Pa. A crater formation process was taken by an image-converter camera every 5 μ s, and 18 successive images were obtained for each shot. From these images, we examined the characteristics of impact eject such as the growth rate, and the shape, and it was compared with that of pure ice. We measured the crater shapes by a caliper.

We found that the spallation was difficult to occur on the ice-rock mixture targets compared to pure ice targets. So, the depth-diameter ratio of the crater for ice-rock mixtures, these dependencies on the velocities, and the projectile densities was different from that of pure ice targets. We found that the crater diameter on the ice-rock mixture is about a half of that on pure ice at the same impact energy. Hiraoka et al. (2004) made the cratering experiments on ice-rock mixture with the rock contents from 0 to 50 wt% at the constant impact energy. We compared their results with our results obtained for 80 wt% and found that our result is almost consistent with their results of 50 wt% content. This means that the crater size stop decreasing at 50 wt%, then it becomes almost constant until 80 wt%. We speculate that the crater size might drastically change to be small between 80 to 100 wt% corresponding to rock itself. It might be possible that the crater size could be controlled by the ice strength from 0 to 80wt% and by the rock strength at the range of content near 100 wt%. The crater scaling law proposed by Housen and Holsapple (2012) was applied, and the scaled crater radius π_R and the scaled strength π_Y were investigated in our results. Our results were compared with that of pure ice and the ice-rock mixture's dynamic tensile strength was supposed to be 100MPa if the ice-rock mixture was scaled by the same parameter as that of pure ice.

Keywords: icy satellites, ice-sand mixture, impact crater, high velocity impact experiments

Experimental study on the decay process of impact-induced stress propagating through granular materials

MATSUE, Kazuma^{1*}; ARAKAWA, Masahiko¹; YASUI, Minami²

¹Graduate School of Science, Kobe University, ²Organization of Advanced Science and Technology, Kobe University

Introduction: Impact process is one of the most important physical processes in the solar nebula. In order to understand the impact histories related to planetary formation process, it is important to study the impact cratering process and the scaling law. Impact cratering experiments have been performed on granular material, and the crater size is found to be different depending on the target material. So, it is necessary to study how physical properties affect the cratering process, especially for excavation stage. Excavation flow is a main process that controls the crater size, so we should examine the effects of material properties. However, it is difficult to observe the flow inside the target, so we used the in-material sensor to measure the pressure. The pressure distribution in the granular target would show the flow and we can compare the crater size and the pressure distribution to clarify the effect of target materials on the crater formation process.

Experimental method: We prepared a target container with a pressure sensor to measure the stress generated by impact. It is made of aluminum with the size of 10cm×10cm×10cm, and we changed the depth of the granular target from 1 to 10cm. The pressure sensor (20kPa, ≤2kHz) was attached on the bottom of the container just below the impact point, and impact experiments were conducted by a free-fall or by a one-stage vertical He-gas gun in Kobe University. We studied the effects of projectile size and impact velocity on the crater size and the stress wave. We used glass beads and quartz sand with the diameter of 100 and 500μm as granular target, and glass balls ($\phi=7.75, 10, 15\text{mm}$) in free-fall, nylon and alumina ($\phi=3\text{mm}$) in vertical gun experiments as projectile. Impact velocity is 2-5.5m/s in free-fall and 60-70m/s in vertical gun experiments. We observed crater size and pressure wave in each experiment.

Results: We found that the size of the impact crater strongly depends on the granular materials, that is, the crater formed on the quartz sand was systematically smaller than that formed on the glass beads. Then, we found that the pressure wave increased suddenly and decreased with a relaxation time depending on target materials. The relaxation time is small for quartz sand and long for glass beads, and the relaxation time of 100μm quartz sand was not measured because of normal mode oscillation of the pressure sensor: it means that the time is less than 0.5ms.

Although the normal mode oscillation of the sensor was observed in the high velocity impact and the shallow depth impact in the case of gas gun experiments, we analyzed the peak of measure pressure waves (P_{max}) and obtained the relaxation time (τ) by fitting them with the following function: $P(t)-P(\infty)=A\exp(-t/\tau)$, where t is time after the impact. As a result, τ is obtained to be 1ms for glass beads target irrespective of the bead size, and 0.1ms for 500μm quartz sand. The relationship between the pressure and the propagation distance was described by $P(r)=P_0(r/L)^{-b}$, where L is a projectile radius, r is distance, P_0 is an initial impact pressure, and b is a decay constant. The decay constant was found to change with the impact velocity and the target materials: it was derived to be 0.79, 0.94 in a low velocity range, 1.61, 1.71 in a high velocity range for glass beads, quartz sand.

We found that the relationship between the crater size and P_{max} at 4cm depth was different in each granular material. The crater size of the glass beads target was larger than that of the quartz sand at the same P_{max} . Then, we introduce a new parameter expressed by τ times P_{max} , so called impulse, I . We renewed the relationship using I instead of P_{max} and found that all data set were merged on one line. This means that I could be a suitable parameter to describe the material dependence of the cratering efficiency. We would like to clarify what material properties determine the τ and how it changed with the physical condition in the future.

Keywords: Excavation flow, Granular material, Cratering process

Effects of impact angles on the impact strength of icy and rocky planetesimals for the collision among equal size bodies

KOMOTO, Yasunari¹ ; ARAKAWA, Masahiko¹ ; YASUI, Minami^{2*}

¹Graduate School of Science, Kobe University, ²Organization of Advanced Science and Technology, Kobe University

Introduction: There are a lot of impact experiments to simulate planetesimals collisions, and most of them had a large mass difference between a projectile and a target. The impact strength is well known that they are described by the energy density: the ratio of the projectile kinetic energy to the mass of the target and the projectile. So, when the projectile is rather smaller than the target (this is an usual situation in the lab. experiments), the very high speed more than 1 km/s is necessary to disrupt the target. This is an analogy of the present asteroid collisions, but it might be far from the simulation expected in planetesimals collisions. Because we speculate the collisions among the similar size small bodies in the solar nebula, and the relative collisional velocity among them could be several 10 m/s. Therefore, it should be important that the planetesimals were disrupted or not at the impact speed around several 10m/s for the collisions among similar size small bodies, then we must conduct the collisional experiments to derive the impact strength of planetesimals in the similar size collisions. In this study, we carried out the impact experiments using the equal size ball made of ice, gypsum, and gypsum-glass beads mixture. These samples simulate icy planetesimals, planetesimals for chondrite parent bodies. We also conducted not only head-on collision but also oblique collision and studied the effects of impact angles on the impact disruption.

Experimental methods: We prepared three types of ball sample with the size of 25 mm and 30 mm made of ice, gypsum-glass beads mixture, and gypsum. They were made by putting each solution in a round mold to form spherical sample. The impact experiments were made by using three types of accelerators: they are a spring gun for low velocity collision, a vertical gas gun for ice and a horizontal gas gun for gypsum, and the achieved velocity is from 4 to 160m/s. The oblique impact was also conducted by shifting the impact point from the geometrical center of the target. The impact angle was changed from 0 deg. (normal impact) to 80 deg. (nearly passing away impact). Impact experiments were observed by a high-speed camera and all of the impact fragments were collected to measure the weight and establish the size distribution. We looked for the recovered fragments to identify the same fragment found in the video image, and tried to construct the velocity-mass distribution of the impact fragments.

Results: We used the reduce mass to calculate the impact energy in the center-of-mass system, so the energy density Q_g was defined by the ratio of the kinetic energy of two bodies in the center-of-mass system to the mass of the two equal balls. The impact strength was obtained for the similar size collisions by using this Q_g . As a result, the impact strength Q_g^* of ice and gypsum was derived to be almost similar to that obtained for the impact experiments with the mass difference more than 10. However, the Q_g^* of glass beads-gypsum mixture was derived to be rather smaller than that obtained in the previous experiments. In the oblique impacts, the mass of the maximum impact fragment was found to decrease with the increase of the impact angle. So, we modify the energy density by using the velocity component normal to the impact surface which effectively work for the disruption, then this modified energy density enabled us to fit all of the data on one line for each target. Finally, we estimated the re-accumulation condition of planetesimals according to the velocity distribution of the impact fragments that obtained in this study. As a result, it is speculated that icy planetesimals could re-accumulate for the bodies larger than 20 km in the diameter, and this threshold size for the planetesimals of ordinary chondrite parent bodies is 5.2km and that for the planetesimals of carbonaceous chondrite parent bodies is 6.7km.

Keywords: Planetesimals, Oblique impact, Impact strength, Energy partition, Re-accretion

Dynamic compaction experiments of porous materials: Implications for impact compaction of pre-planetesimals

YASUI, Minami^{1*}; YOKOTA, Mizuki²; SAKAMOTO, Kana²; ARAKAWA, Masahiko³

¹Organization of Advanced Science and Technology, Kobe University, ²Faculty of Science, Kobe University, ³Graduate School of Science, Kobe University

Introduction: Two theories are proposed for the growth mechanism of bodies with the diameter from cm to several hundreds meters (pre-planetesimals). One is that planetesimals could form by a gravitational instability in the dust layer of a protoplanetary disk. The other is that planetesimals could form by a repeating impact coagulation of dust aggregates. In this study, we focus on the latter theory. There are some problems that planetesimals could not grow because of rebound and catastrophic disruption among pre-planetesimals caused by the increase of average density. Sakamoto (2013) did free-fall impact experiments of porous snow simulating icy pre-planetesimals by using the stainless cylinder to examine the compaction conditions, and clarified the relationship between the impact stress and the final density profile and the size of compaction area. However, the impact velocities in her study were 0.7 to 3.5 m/s, relatively lower compared to the average impact speed of pre-planetesimals. In this study, we conducted impact experiments of porous materials at >5 m/s to examine the compaction mechanism, impact stress, and density profile.

Experimental methods: The target was high porous snow with the initial porosities of 70 and 80% and perlite particles with the density of 85 kg/m³ simulating the icy and rocky pre-planetesimals. We did impact experiments of snow in the cold room (-10 °C) at ILTS, Hokkaido University, and perlite at Kobe University, by using the one-stage vertical and horizontal light gas guns. The vertical gun was used for only snow targets. The target was prepared by packing ice grains or perlite particles into the acrylic tube, up to 120 mm depth, and the blue ice grains or the red perlite particles were put into the target every 20 mm from the bottom due to measure the density changing with depth. The piston was set on the target surface in the acrylic tube, and accelerated by the projectile to compress the target. The projectiles were an elastic ball with the diameter of 25 mm for horizontal gun and same ball installed on the cylindrical sabot with the diameter of 30 mm for vertical gun. The pistons were a polycarbonate, an aluminum, and a polyacetal cylinders with the diameter of 30 mm and the height of 10-30 mm to examine the effects of piston type. The impact velocities were 2-118 m/s. The impact compaction of the target was observed by a high-speed digital camera. The shutter speed was set to be 20 to 100 μ s, and the frame rate was set to be 6000 to 10000 fps.

Results: First, we measured the impact stress from the motion of piston, σ_p , and compared σ_p with the strength calculated by Kinoshita method, Y . As a result, the σ_p was almost same with the Y for both perlite and snow targets.

Next, we measured the final density of target, ρ_f , and obtained the relationship between the ρ_f and the kinetic energy or the momentum of projectile. As a result, we found that the ρ_f for perlite was determined by the kinetic energy while that for snow was determined by the momentum. Furthermore, we proposed the model of ρ_f for perlite and snow by assuming these compaction mechanisms: the perlite compressed due to the fracture of perlite particles while the snow compressed due to the decrease of area among ice grains. We compared these models with our experimental results and found that they were almost consistent with each other.

Finally, we examined the relationship between the σ_p and the final density of top layer in the target, ρ_{f1} . As a result, we obtained as $\rho_{f1}=3.0\sigma_p^{0.8}$ for perlite and $\rho_{f1}=127\sigma_p^{0.3}$ for snow in kPa. The data for snow at $\sigma_p >100$ kPa was scattered because the compaction mechanism was changed at $\sigma_p >100$ kPa.

Keywords: pre-planetesimal, dynamic compaction, impact experiment, final density, Kinoshita strength, compression viscosity

Effect of particle size distribution on thermal conductivity of powdered materials

SAKATANI, Naoya^{1*} ; OGAWA, Kazunori² ; HONDA, Rie³ ; ARAKAWA, Masahiko⁴ ; TANAKA, Satoshi²

¹The Graduate University for Advanced Studies, ²Institute of Space and Astronautical Science, ³Kochi University, ⁴Kobe University

Understanding about heat transport mechanism of powdered materials, such as lunar surface regolith, is important issue in order to estimate planetary thermal evolution and present thermal state. Thermal conductivity of powdered materials depends on various parameters (particle size and its distribution, temperature, compressional stress, etc.). Depending on these parameters, thermal conductivity can vary by one order of magnitude. Due to insufficiency of the experimental studies, heat transfer mechanism is not understood enough, and it is difficult to constrain in-situ thermal conductivity on planetary surface.

Our purpose is to understand the heat transfer mechanism of powdered materials under vacuum conditions by means of systematic survey of parameter dependences of the thermal conductivity. This will enable us to model the thermal conductivity, which can apply the estimation of thermal conductivity structure on planetary surface. Most of previous studies focus on the powdered samples with uniform particle size. However, actual planetary regolith has wide range of particle size from sub- μm to mm. Moreover, parent bodies of chondritic meteorites would be composed of mixture of meteoritic matrix and chondrule. In this presentation, we will report the effect of particle size distribution on the thermal conductivity under vacuum.

Glass beads mixtures of 100 μm and 200 μm in diameters were used. Prepared samples had volume mixing ratio of 1:0, 2:1, 1:1, 1:2, and 0:1. Porosity of each sample was 0.38, 0.35, 0.32, 0.35, and 0.38, respectively. The thermal conductivity of these samples was measured by line heat source method.

As a result, 100 and 200 μm glass beads of uniform sizes had 0.0023 and 0.0035 W/mK, respectively. This difference in the conductivity would be caused by the difference of radiative heat transfer. On the other hand, mixing samples had thermal conductivity of 0.0039, 0.0029, and 0.0039 W/mK for mixing ratio of 2:1, 1:1, and 1:2, respectively. These conductivities related well to porosity. There were no linear relation between thermal conductivity and mixing ratio. We found M-shaped correlation between them.

The measured thermal conductivity can be represented by the sum of solid conductivity, which is conductive contribution through contact area between the particles, and radiative conductivity, which is radiative contribution through the pore between the particle surfaces. Our results will be explained by the variation of these conductivities with particle size distribution. Therefore, it is necessary to separate the measured values into solid and radiative conductivities for explanation of our experimental results. This can be accomplished by investigation of temperature dependence of the conductivity. In this presentation, we will report dependence of solid and radiative conductivities on the particle size distribution.

Measurement experiments of thermal conductivity and sound velocity in sintered glass beads

TSUDA, Shoko¹ ; OGAWA, Kazunori^{1*} ; SAKATANI, Naoya² ; ARAKAWA, Masahiko³ ; YASUI, Minami³

¹The University of Tokyo, ²The Graduate University for Advanced Studies, ³Kobe University

The thermal conductivity and sound velocity of sintered particle materials (glass beads) were experimentally measured, and a correlation between them was investigated. Particles have often played important roles in the solar system history. Especially dust particles condensed in the early solar nebula formed planetesimals, and they remained as the main structure material of the bodies. The particles were then gradually sintered as temperature increased by disintegrations of radioactive isotopes. Finally, a part of planetesimals might be completely sintered and began to melt. Currently the sintered materials may also exist on the lunar and asteroid subsurface for example. Mechanical and thermal properties of such sintered materials are essential information for investigating the history of these bodies.

In the thermal issues, particles are known as a strong thermal insulator in vacuum. Although the thermal conductivity of sintered materials has never been measured, it is considered to be a value between the unsintered and a continuous rock, depending on degree of the sintering process. Concerning the sound velocity, characteristic feature depending on the sintering degree is expected to be similar to the thermal conductivity, because basically the phonon conduction is a common mechanism for both the thermal and sound phenomena in electrical insulation materials.

In this presentation, we report results of the first experiments of the thermal conductivity and sound velocity measurements in sintered particle materials. For measurement samples, 9 different blocks of sintered soda-lime glass beads were prepared: three bead diameters of 180-255, 355-500, and 710-1000 μm , and three degrees of sintering that have nearly the same porosity 40%. The cross section of sintering contact sites (neck) was evaluated for each sample. The thermal conductivity was measured by the line heat source method by a line heater and temperature sensors given in the sample in advance. The sound velocity was directly measured by a transmitter and receiver put at both ends of the block samples.

As results of the experiments, both the thermal conductivity and the sound velocity had an apparent correlation with each other, and with degree of sintering. They appeared almost in proportion to the neck diameter, which feature obviously indicates that the neck or contact size controls the bulk thermal and sound conductions, in weakly-sintered particle systems at least. These results can be directly applied to estimation of thermal and mechanical property of the ancient planetesimals. These results also suggest that the thermal conductivity of sintered materials, and also of unsintered particles probably, can be evaluated by measurements of the sound velocity.

Keywords: Particle material, Regolith, Thermal Conductivity, Sound velocity, Glass beads

Experiment to know the power to pull mutually between things that are axisymmetric for the Saturn's-like magnetic axis

MASE, Hirofumi^{1*}

¹none

The magnetic axis of magnetic field in the Saturn is corresponding to the rotation axis(1). And, Saturn's rings revolve on the equatorial plane of the Saturn(2). I want to think that the reason why beautiful rings exist miraculously is related to these miraculous features. The power to pull against each other between things that are axisymmetric for the magnetic axis is generated on the plane that passes center of the axial dipole field and intersects vertically for the magnetic axis. Because the material that composes the ring is tied to the material on the 180-degree other side by the surcharge-gravitation, Saturn's rings are generated and maintained. I am making the experiment that proves the truth of this hypothesis. I introduce the result of it.

****Composition of experiment (Please refer to the drawing)**

"A","C":the one(34L*25W*25H) that natural whetstone(sandstone) was cut

"B":the one(40L*40W*40-80H) that 4-8 pieces of permanent magnet(anisotropic ferrite,40L*40W*10H,B=79mT,F=2.746kgf)s were piled up

Device box:I used "two step box" on the market and remodeled it. The front side of the left cell of this box is glazed. The front side of the right cell of this box is opening. Plywood in which "B" is set is put on the medium plate of this box to close the hole in the plate. The left cell is airtight exclusive of the top of the vinyl chloride pipe. "A" is hung from the ceiling by two strings(1,700L) and can swing freely in the left cell. The space of "B" and "A" in geostationary point is about 20mm. "C" is hung from the top board in the right cell by the string. The edge of another string is bonded on the right side of "C". (State:"C1")"C" can be separated from "B" by pulling this string from the right side of this box. (State:"C2")"C" can approach "B" by loosening this string.

****Condition of experiment**I experimented on the following three kinds of by changing the composition and direction of "B". Condition 1:pile 8 pieces vertically(magnetic axis is perpendicular) Condition 2:pile 4 pieces vertically(axis, perpendicular) Condition 3:pile 4 pieces horizontally(axis, horizontal right and left)

****Procedure of one experiment**1.I wait as much as possible until the swing of "A" stops(now"C1"). 2.I begin taking a picture of the animation of "A" with the video camera(now"C1"). 3.After 2 minutes pass, I change State from "C1" into "C2"(now"C2"). 4.After 4 minutes pass, from "C2" into "C1"(now"C1"). 5.After 6 minutes pass, from "C1" into "C2"(now"C2"). 6.After 8 minutes pass, I end taking a picture.

****Result of experiment**"A" swung faintly when taking a picture was begun. 1.In case of Condition 1 and 2, the swing was controlled at time zone in State "C2" of the first times, and was amplified at time zone in State "C2" of the second times. 2.In case of Condition 3, I could not confirm special change of "A" during all time.

****Consideration**I seem I can conclude that static electricity and magnetism don't influence the result by the comparison between Condition 2 and 3. There is a possibility that the power that I had expected was detected.

Reference literature

(1)Hori/"The School of the Universe (13th)"/NAOJ

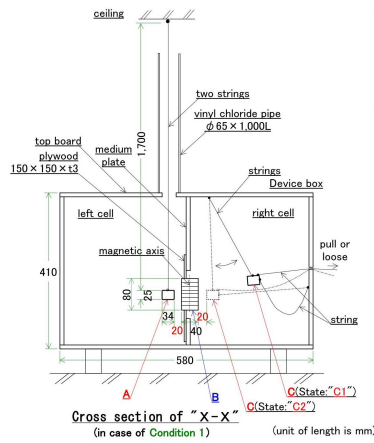
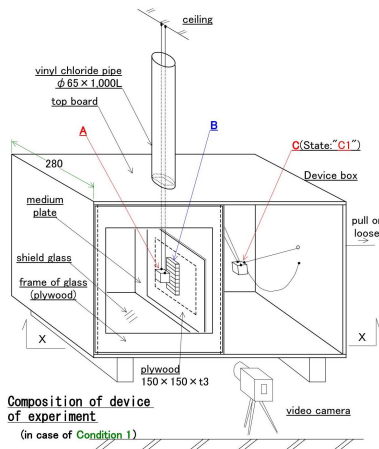
http://th.nao.ac.jp/MEMBER/hori/pdf/HORI_2013Mar26_part1.pdf P23

(2)Hiratsuka City Museum http://www.hirahaku.jp/hakubutsukan_archive/tenmon/00000050/59.html

PPS21-P20

Room:Poster

Time:April 29 18:15-19:30



A, C: natural whetstone(sandstone)
 34L x 23W x 23H
 B: permanent magnet(anisotropic ferrite, 40L x 40W x 10H,
 B=79mT, F=2.746kgf) piled up 4~8 pieces
 40L x 40W x 40~80H

